Visual acuity in pelagic fishes and mollusks

Yakir L. Gagnon, Tracey T. Sutton, and Sönke Johnsen

July 7, 2015

Abstract

In the sea, visual scenes change dramatically with depth. At shallow and moderate depths (< 1000 m), there is enough light for animals to see the surfaces and shapes of prey, predators, and conspecifics. This changes below 1000 meters, where no downwelling daylight remains and the only source of light is bioluminescence. These different visual scenes require different visual adaptations and eye morphologies. In this study we investigate how the optical characteristics of animal lenses correlate with depth and ecology. We measured the radius, focal length, and optical quality of the lenses of pelagic fishes, cephalopods, and a gastropod using a custom-built apparatus. The hatchetfishes (*Argyropelecus aculeatus* and *Sternoptyx diaphana*) and the barrel-eye (*Opisthoproctus soleatus*) were found to have the best lenses, which may allow them to break the counterillumination camouflage of their prey. The heteropod lens had unidirectional aberrations that matched its ribbon-shaped retina. We also found that lens angular resolution increased with depth. Due to a similar trend in the angular separation between adjacent ganglion cells in the retinas of fishes, the perceived visual contrast at the retinal cutoff frequency was constant with depth. The increase in acuity with depth allows the predators to focus all the available light bioluminescent prey animals emit and detect their next meal.

Introduction

The ocean is a challenging environment for visual animals. Downwelling light gets quickly absorbed and scattered by the water and illumination decreases

exponentially with depth becoming almost completely blue after ~ 50 meters (Lythgoe, 1979). At epipelagic depths (0–200 m), the monochromatic downwelling light illuminates objects creating extended scenes – targets with a visible surface area. Many complex adaptations have evolved to detect prey, predators, and conspecifics in this relatively illuminated zone. These include polarization vision (Waterman, 1981), ultraviolet vision (Browman et al., 1994, Bowmaker and Kunz, 1987), colored ocular filters (Muntz, 1976), and offset visual pigments (Lythgoe, 1984, Loew et al., 1993). At mesopelagic depths (200–1000 m) some predators hunt by searching for prey silhouetted against the dim downwelling light using their large upward-facing eyes (Muntz, 1990, Warrant et al., 2003). Below 1000 meters, downwelling light is not bright enough to see. At these bathypelagic depths (> 1000 m), bioluminescence is more common and the visual scene is dominated by point sources with no visible surface area (although some medusae, ctenophores, and siphonophores may be considered as extended bioluminescence sources). Not much is known about the visual adaptations in this depth zone. However, recent studies have shown that bathypelagic fishes have surprisingly high anatomical acuity in their specialized foveae (the region where ganglion cell density is the highest in the retina) (Wagner et al., 1998, Warrant, 2000). The importance of vision to bathypelagic fishes is emphasized by the energetic cost required to maintain high visual acuity (Laughlin et al., 1998), despite the scarcity of available nutrients. However, the amount of information that reaches their retina is initially limited by the optical quality of their lenses.

In aquatic vertebrates, the cornea is surrounded by water on the outside and watery aqueous humor on the inside, both of which have similar refractive indices. In contrast to terrestrial corneas which are surrounded by air on the outside, the refractive power of most aquatic corneas is therefore negligible (Mandelman and Sivak, 1983, Matthiessen, 1886). Cephalopods have circumvented the cornea altogether: their lenses are in direct contact with the surrounding water. In both cases, the task of focusing light on the retina is thus left to the lens alone. In order to maximize refractive power, aquatic lenses are typically spherical in shape (Pumphrey, 1961, Sivak and Luer, 1991, Walls, 1942). In addition, spherical lenses need to be gradient-index lenses (i.e. have a radially symmetrical refractive index gradient) to minimize longitudinal spherical aberrations (Maxwell, 1854). A lens' aberration and its optical quality can be quantified by measuring the lens' Point Spread Function (PSF) – which can be represented by imaging a point source after

it has been focused by the lens. An ideal lens would focus the rays emitted from the point source to an identical point on the other side of the lens. The size of the focused point depends on the aperture due to diffraction but also on the optical quality of the lens. The distribution of light intensities at the focused point characterizes the lens' aberrations.

Many animals integrate the signals from multiple adjacent retinal ganglion cells to increase their eyes' sensitivity in dim environments. This is known as spatial summation (Land and Nilsson, 2002, Warrant and Locket, 2004). However, in an environment where most of the visual cues are point sources (i.e. not extended scenes), spatial summation will not increase sensitivity because the light falls on one photoreceptor (Warrant, 1999). It is therefore believed that the image of a point source focused by a lens of a deep-sea animal should not be larger than the receptive field of its retinal ganglion cells (Warrant, 2000). Because bathypelagic fishes are known to have smaller angular separation between adjacent ganglion cells in their retina (and therefore higher anatomical acuity) than shallow dwelling fishes (Wagner et al., 1998, Warrant, 2000), it follows that fishes living in deeper waters should have lenses that are capable of resolving finer (angular) details than fishes living in shallower waters.

The effect of lens quality on the visual acuity of pelagic animals is unknown. We therefore measured the lens PSF, radius, and focal length of 24 fish species, five cephalopods, and one heteropod using a custom-built apparatus. These species inhabit a wide range of depths, from bright shallow epipelagic waters down to dark bathypelagic depths. By quantifying the optical quality of each species' lens we hoped to understand how each lens is adapted to its respective visual tasks.

Materials and methods

Sample collection

Pelagic fishes and mollusks were collected using an opening/closing Tucker trawl with a 10-m^2 mouth and thermally protecting cod end (Childress et al., 1978) on two separate research cruises on the research vessel *Endeavor* off the coast of Rhode Island (RI), USA (mainly in two locations $37^\circ\,0'\,8''$ N, $71^\circ\,11'\,41''$ W and $38^\circ\,34'\,56''$ N, $67^\circ\,57'\,53''$ W – also known as "Oceanographer Canyon" on September 19^{th}–30^{th}, 2011) and on the research vessel *Kilo*

Moana outside Hawaii (HI) (21° 30′ 36″ N, 157° 30′ 6″ W on May 30$^{\text{th}}$–June 9$^{\text{th}}$, 2011). Lenses were dissected out of the eyes and analyzed immediately after euthanization of the animal by rapid decapitation and pithing.

Point spread function measurements

Each animal lens' point spread function (PSF) was created and characterized by shining monochromatic collimated light through the excised lens and imaging it on a Charge-Coupled Device, CCD (Figure 1). A tungsten-halogen light source (LS-1, Ocean Optics Inc., Dunedin FL, USA, 360–2500 nm) was directed through a 100 μm diameter optical fiber and collimated by an achromatic collimating lens (74-ACR, Ocean Optics). The beam of light passed through a 550 nm bandpass interference filter with a Full Width at Half Maximum (FWHM) of 10 nm (all optical components were from Edmund Optics, Barrington, NJ, USA). Collimated light entered a plastic chamber ($29 \times 29 \times 20$ mm) filled with phosphate buffered saline (PBS) through a calcium fluoride window, refracted through the animal lens, and exited the chamber through a thin transparent PVC film ($\sim$ 10 μm). The film was adjacent to and in contact with the CCD of an AVT Guppy Pro F-503 monochrome camera. The distance between the collimating lens and camera CCD was 80 cm and the divergence angle of the beam was 10 mrad. The setup was mounted on a bench plate placed on a rubber sheet and double-cam leveling feet to minimize vibrations due to the ship's movements and engine.

The animal lens was held in place by gluing (Super Glue) its suspensory ligaments and retractor lentis muscle to a metal pin connected to a translation stage. This stage moved the lens along the optical axis of the system to increase or decrease the lens' paraxial distance to the CCD while the camera recorded the PSFs (the camera's response was linear). All the positions of the stage were recorded and used to measure the distances between the CCD and lens center – image distances. This resulted in a sequence of 100–400 monochrome images (640×480 pixels in UINT16 class, i.e. 65536 gray levels) and image distances per lens.

Parameterization

The resulting images depict the three-dimensional PSF of the lenses (see Figure 2 for an illustration of the following procedure). While this is practical

for image analysis, it is too complex for comparisons of lens quality between species. A more effective approach is to calculate the PSF's full width at the mid point between its smallest and largest values – this value is known as the Full Width at Half Maximum (FWHM) and is useful as an estimate for the function's spread (Figure 2). Lenses with a small FWHM produce sharp images while large FWHM result in blurry images. The effect a lens has on a point source can be approximated with a three-dimensional Gaussian function that is symmetrical about its optical axis. Therefore, the diameter of the circle surrounding the PSF at mid height is the PSF's FWHM. To calculate the FWHM in this study, we subtracted the mode (the most frequent value in a dataset) of each PSF image from the image to remove any electric noise the CCD might have had and background illumination that would have contaminated the image (all image and data analysis were done in Matlab R2011b, Mathworks Inc., Natick, MA). Next, the number of pixels that had intensities greater than half the maximum value in each image was calculated – this value equaled the area of the circular cross section of the three-dimensional PSF at half its height. Lastly, the diameter of this circle was calculated to determine the PSF's FWHM and was equal to twice the square root of the area divided by π.

In addition to measuring the FWHM in μm, the angular FWHM ($\angle$FWHM) was also calculated. Angular distance can be defined as the angle between the optical axis and the line between the system's nodal point (the lens center) and the point where the light hit the CCD. We therefore calculated the $\angle$FWHM as double the arcsin of the FWHM divided by the focal length. The $\angle$FWHM is useful because it removes differences in scale when comparing differently sized eyes. Finally, the lenses' f-number, $f/\#$, which is the ratio between the lens' focal length and diameter, was calculated.

Since the suspensory ligaments and retractor lentis muscle shift the fish lens when accommodating in the living fish eye (Khorramshahi et al., 2008), it is difficult to assess the fish's accommodative state. It is however safe to assume that the retina is located at the focal-plane (i.e. where the 'most focused' image is formed). We defined the focal-plane as the PSF with the smallest FWHM. The distance of the image with the smallest FWHM was therefore chosen as the lens' focal length for both fishes and mollusks.

The variation of the PSF's FWHM within a given species in this study is affected by a number of factors. There are, however, more factors increasing the FWHM than there are decreasing it. An increase in FWHM is caused by unavoidable lens deterioration during collection. Some of the possible effects

increasing FWHM are trawling in high temperature waters, dissection time, the physiological changes associated with the specimen's death, mechanical stress, and pH and osmolarity differences in the apparatus' chamber. Also, while the lens orientation was controlled by hanging the lens from the suspensory ligament when possible, deviations from that led to off-axis aberrations that would create a broader PSF and thus a larger FWHM. The only reason FWHM would be lower than the population's mean FWHM was not the methods used in this study but the unlikely possibility that we sampled an outlier specimen with unnaturally 'sharp' lenses. Since the risk of underestimating FWHM is smaller than the risk of overestimating it, the lens with the smallest FWHM was chosen as the most representative one for each species.

The PSF of a lens describes its optical quality in the spatial domain. It is however possible to consider the amount of 'blur' a lens introduces in the frequency domain (Figure 2). This is useful because the contrast of a signal can be described at specific spatial frequencies (e.g. number of black and white line pairs per cm). The magnitude (absolute value) of the Fourier Transform of an image of a distant point source taken through a lens results in an image of the lens' Modulation Transfer Function (MTF). This image describes the amount of signal contrast that remained after passing through the lens at different spatial frequencies (denoted by the distance of each pixel from the image-center, where the image center relates to low frequencies and the image periphery relates to high frequencies) and orientations (denoted by the polar coordinates of each pixel). The MTF of each species' lens was calculated and used for assessing the amount of astigmatism (i.e. unequal focus between perpendicular signals) in the lens.

The effect of depth on lens optical quality

The regression of the lens radius, focal length, $f/\#$, FWHM and $\angle$FWHM against the animals' mean daytime depth was investigated. Some of the fish depth data were taken from www.fishbase.org (2012) through the R package (R version 2.15.2) *rfishbase* (Boettiger et al., 2012) while the depth data for all other animals were obtained from various sources (see Table 1 for details). Linear regression models were fitted to the data (all statistic analysis was done in R). Since the light environment below 1000 m depth is relatively homogeneous (Jerlov, 1976), we assumed that the lens optics of animals living at depths greater than 1000 m should have very little variation and therefore set all mean depths larger than 1000 m to 1000 m in the linear

regression. Another factor affecting the optical properties of pelagic animals' visual systems is the extent of the animal's depth range. While animals with a narrow depth range might be suited to their mean depth, animals with a similar mean depth but broader depth range may exhibit properties found in both shallower as well as deeper dwelling animals. In order to accommodate for this discrepancy, the mean depth regressor was weighted by the inverse of the width of the animals' depth range (depth ranges were first categorized into five size categories).

Contrast

The contrast of maximally resolved signals (i.e. the finest details a system can resolve) in camera-type eyes can be calculated using two ocular characteristics: 1) the lens' MTF and 2) the retina's cutoff frequency, which is the maximal spatial frequency the retina can resolve (i.e. its resolution). Assuming the lens PSF is a Gaussian function with a standard deviation of σ, the contrast of signals at the retina cutoff frequency, ν_0, is equal to:

$$C_0 = \exp -\tfrac{1}{2} \left(\nu_0 \sigma\right)^2 . \tag{1}$$

This equation depends on two variables: the standard deviation of the (Gaussian) PSF, σ, and the retina cutoff frequency, ν_0. The PSF standard deviation is equal to the $\angle$FWHM divided by $2\sqrt{2\log 2}$, and the cutoff frequency of the retina is equal to half the inverse of the angular separation between adjacent ganglion cells in the retina (Land and Nilsson, 2002). In order to predict how the contrast of a viewer changes with depth, σ was calculated from the $\angle$FWHM regression. The same linear regression analysis as described before was used on the interganglion angles from Wagner et al. (1998) (slightly amended on five accounts with original author's approval). Wagner et al. (1998) measured the interganglion angles of 21 mesopelagic and bathypelagic fish species. The linear models for $\angle$FWHM and interganglion separation angles were used in Equation 1 to predict how the contrast of maximally resolved signals changes with depth. In order to calculate the 95% confidence intervals of the prediction, the variance-covariance matrix of the two linear models were used.

Results

The number of replicates (animals and lenses), mean and standard deviation of the lens radius, focal length, and $f/\#$, as well as the narrowest FWHM, smallest ∠FWHM, and depth range are summarized in Table 1. In bony fishes (24 species), the smallest lenses belonged to the bathypelagic gulper (*Saccopharynx* sp.), and the largest to the epipelagic flying fish (*Cheilopogon* sp.). The snipe-eel, *Avocettina infans*, had the shortest focal length (the gulper's focal length was not measured successfully) and the barrel-eye *Opisthoproctus soleatus* the longest (note that the flying fish's focal length would most probably have been longer, but due to the experimental chamber's size it was not measured). The ratio between the focal length and lens diameter ($f/\#$) varied between 0.78 (*Coccorella atlantica*) and 1.6 (*Regalecus glesne*). The oarfish's (*R. glesne*) exceptionally large $f/\#$ might have to do with the fact it was a juvenile (the specimen body length was relatively short, $\sim$ 9 cm). Teleost $f/\#$ is known to be inversely proportional to age (Shand et al., 1999) (the three next largest $f/\#$ belonged to *Anoplogaster cornuta*, 1.3, and *Argyropelecus aculeatus* and *O. soleatus*, 1.2). The narrowest PSF had a FWHM of 4.3 μm and was found in *Avocettina infans*, *Benthosema suborbitale*, *Gonostoma elongatum*, and *Sternoptyx diaphana*. The gulper had the widest FWHM (74 μm). The smallfin lanternfish (*B. suborbitale*) had the narrowest ∠FWHM, 0.08° while *Caranx bartholomaei* had the broadest, 0.38°. For comparison, the lens of a rainbow trout (*Oncorhychus mykiss*) has an ∠FWHM of 0.06° (Jagger, 1996). Of all the cephalopods (five species), *Pterygioteuthis microlampus* had the smallest lens, focal length, $f/\#$, and FWHM. *Sthenoteuthis oualaniensis* had the largest lens, focal length, and $f/\#$ as well as the smallest ∠FWHM. *Chiroteuthis* sp. had the largest FWHM and *Illex* sp. the largest ∠FWHM.The heteropod mollusk *Pterotrachea coronata* had one of the narrowest FWHM (3.5 μm) from all the studied species in this study. The Chordate lenses were not significantly different from the Molluscan ones in any of the lens parameters measured in this study (two-sample t-test P $\gtrsim$ 0.50).

The PSFs for a selection of species are shown in Figure 3. While most PSFs are approximately rotationally symmetrical (e.g. *Diplospinus multistriatus* in Figure 3), some lenses displayed aberrations such as coma and astigmatism (e.g. *Idiacanthus antrostomus* in Figure 3). These aberrations are expressed as an ellipsoid distribution of intensities in the MTFs (Figure 4). While some of the aberrations were small and resulted in circularly shaped MTFs

– *Malacosteus niger* and *Astronesthes lucifer*'s MTF in Figure 4 – the heteropod *Pterotrachea coronata* had one of the most elliptically shaped MTFs.

The linear regression was significant for ∠FWHM (the slope was $-0.14 \cdot 10^{-3}$, P = 0.017 for 25 species) and lens radius ($a = -2.5 \cdot 10^{-3}$, P = 0.015, $n = 30$) as a function of mean daytime depth (Figure 5). However, the flying fish' shallow depth and large lens affected the lens radius regression heavily and the significance disappeared after its removal (P = 0.47). The linear regression was not significant for focal length (P = 0.76, n = 25), $f/\#$ (P = 0.85, n = 25), or FWHM (P = 0.29, n = 30). These results indicate that animals living deeper have narrower ∠FWHM. The regression of interganglion cells was significant (P = 0.032 for 21 fish species) and indicated that interganglion separation angles decreased by $-0.061 \cdot 10^{-1}$ degrees per 100 meters depth (Figure 5). Contrast was constant at 60% for all depths (Figure 5) indicating that the lenses' angular focus matched the angular resolution of the retinas at all depths.

Discussion

Optical quality

The optical qualities of lenses in this study were well adapted to the species' lifestyle. Fishes with large upward-facing eyes are believed to hunt for prey by detecting silhouettes against the dim downwelling light (Muntz, 1990, Warrant et al., 2003). Many of their prey use counterillumination to hide their own shadows. The discrete bioluminescence-emitting photophores are usually unevenly spaced on the ventral side of the camouflaged animal and could potentially be detected by viewers that have sufficient visual acuity (Johnsen et al., 2004). The hatchetfish *A. aculeatus* and *S. diaphana* as well as the the barrel-eye *O. soleatus* have pronounced upward-facing eyes. Stomach contents show that the hatchetfishes have a varied diet that includes copepods (e.g. Pleuromamma, and Oncaea), ostracods, small fish, and molluscs (Hopkins and Baird, 1985). The bioluminescence of many of these prey items is chromatically similar to the downwelling light (Latz et al., 1988, Herring et al., 1993, Haddock and Case, 1999). The barrel-eye primarily preys on bioluminescent (Haddock and Case, 1999) siphonophores (Cohen, 1964, Haedrich and Craddock, 1968, Marshall, 1971, 1979). These three fish species have narrow ∠FWHM angles ($\sim 0.1°$) – their lenses are capable of

focusing high spatial frequencies (i.e. small details). These superior optics in combination with high resolution retinas (Collin et al., 1997) may allow these upward viewing predators to break counterillumination camouflage and detect small irregularities in the countershading bioluminescence (Johnsen et al., 2004). The exceptionally narrow FWHM and ∠FWHM of *Avocettina infans*, *Benthosema suborbitale*, *Gonostoma elongatum*, and *Scopelosaurus hoedti* suggest that acute vision is important to these species as well and that they too may use their excellent lenses to break camouflage strategies that are susceptible to sharp vision. For example, ctenophores often include small opaque organs (e.g. retinas and guts) in an otherwise transparent body (Johnsen, 2001, Mayer, 1912, Harbison et al., 1978), and these patches of pigmented or reflective tissue could potentially be visible to viewers with acute vision.

The optical quality of the lenses in this study appeared to be influenced by the mechanical, chemical, and temperature stresses these lenses were exposed to during collection. The distribution of FWHM values for one of the most frequently sampled species (*S. diaphana*) was highly skewed toward lower values with many narrow FWHM and a few wide FWHM 'outliers'. The FWHMs of the holo-bathypelagic fish *Saccopharynx* sp. and the fragile squid *Chiroteuthis* sp. are exceptionally wide (47 and 83 μm respectively) and are probably due to light scattering caused by denaturation of the crystalline proteins in the lens (on the specimen's journey in the trawl-net) rather than naturally low lens resolution. This indicates that even the lowest observed PSF FWHMs might still underestimate the true optical quality of the species in this study. While some of the aberrations visible in the PSFs and MTFs in Figures 3 & 4 may have been caused by these artifacts, most of the optical properties we quantified likely represent the natural state of these lenses. One example of a lens that had an astigmatism aberration that was not caused by methodology was that of the heteropod. The directionally dependent contrast transmittance the heteropod *P. coronata*'s MTF exhibited was apparent in most specimens and fits its morphology exceptionally well. Heteropods have ribbon-shaped retinas which are a few photoreceptors wide and several hundred photoreceptors long (Land, 1982), requiring high quality optics in only one dimension. Heteropods use these 'one-dimensional' eyes to scan the environment one stripe at a time (Land, 1982). Land (1982) found that the photoreceptor width was 3.9 μm in another species of heteropod (*Oxygyrus keraudrenii*) – remarkably close to the FWHM of the lens' PSF (3.5 μm). The directionally dependent optical quality of the heteropod's lens

fits those requirements assuming that in the intact heteropd eye the lens' rotational orientation correlates well with that of the retina. It is remarkable that such a seemingly 'simple' gelatinous animal has such a well tuned visual system.

Matthiessen found that the ratio between lens focal length and radius was roughly 2.5 and constant across many different fish species (Matthiessen, 1882). Our results indicate that deep-sea fish do not follow that rule of thumb. With a mean $f/\#$ (equal to half the Matthiessen ratio) of 1.05, the $f/\#$ were significantly lower than Matthiessen's ratio (one-tailed t-test, $P = 10^{-15}$). The $f/\#$ in this study were not constant either (standard deviation of 0.19). This difference can be explained by the fact that light gathering ability is proportional to the inverse square of the system's $f/\#$ (Land and Nilsson, 2002). Therefore, animals that live in deeper waters and darker environments benefit from lenses with a smaller $f/\#$. The relatively high variation in $f/\#$ may be caused by the large depth range these fish were retrieved from.

The effect of depth on acuity

Visual animals have different contrast requirements when viewing extended scenes in shallow depths than when viewing point sources in deeper waters. An extended scene requires higher contrast than a point source since the number of intensity levels the system needs to differentiate is larger than in a point source scenario: a bright point source on a dark background has just two brightness levels, the source's radiance and zero (for which the inherent contrast is infinite), while the surface of a target may contain any number of brightness levels and may be viewed under any number of physiologically relevant illumination levels. Animals need high contrast images of their environment at shallow depths, but due to the binary nature of the visual scene at bathypelagic depths, a relatively low contrast at the retina cutoff frequency should suffice. Surprisingly, contrast did not decrease with depth – the reason might depend on sensitivity. Since spatial summation does not increase sensitivity at those depths, one of the mechanisms with which these animals can detect small bioluminescent points of light in their environment is aberration-free optics and therefore high contrast. While it is probable that some pelagic species with different acuity and/or sensitivity requirements had either a lower or higher contrast at their retina cutoff frequency than 90%, the general trend seems to show that contrast is not affected by

depth. The ability to resolve finer signals is what increases the eye's resolving power with depth pushing both the retina's and the lens' resolution higher.

In this study, we have shown that pelagic animals have lenses that suit their specific visual tasks. The eyes of hatchetfishes and barrel-eyes had relatively aberrations-free lenses that were suited to hunting for counterilluminated silhouettes, while the scanning eyes of the heteropod had lenses that matched its one-dimensional retina well. Each lens' resolving power was matched to the resolution of the animal's retina, resulting in a constant contrast throughout all depths.

Acknowledgments

We thank Dr. Jules Jaffe's for helpful discussions, Trisha Towanda for supplying the Heteropodes, and Dr Brad Seibel, Dr. Stephanie Bush, and Dr. Sarah Zylinski for general help.

References

Bertelsen, E. and Nielsen, J. (1986). *Fishes of the north-eastern Atlantic and the Mediterranean. volume 2.*, chapter Saccopharyngidae, pages 530–533. UNESCO, Paris.

Boettiger, C., Lang, D. T., and Wainwright, P. C. (2012). rfishbase: exploring, manipulating and visualizing fishbase data from r. *Journal of Fish Biology*, 81(6):2030–2039.

Bowmaker, J. K. and Kunz, Y. W. (1987). UV receptors tetrachromatic color vision and retinal mosaics in the brown trout *Salmo trutta* age-dependent changes. *Vision Research*, 27(12):2101–2108.

Browman, H., Novales-Flamarique, I., and Hawryshyn, C. (1994). Ultraviolet photoreception contributes to prey search behaviour in two species of zooplanktivorous fishes. *Journal of Experimental Biology*, 186(0):187–198.

Childress, J. J., Barnes, A. T., Quetin, L. B., and Robison, B. H. (1978). Thermally protecting cod ends for the recovery of living deep-sea animals. *Deep Sea Research*, 25(4):419 – 422.

Cohen, D. M. (1964). *Fishes of the western north Atlantic, Part 4. Memoir 1*, chapter Suborder Argentinoidea, pages 1–70. Sears Foundation for Marine Research, New Haven, Connecticut.

Collin, S. P., Hoskins, R. V., and Partridge, J. C. (1997). Tubular eyes of deep-sea fishes: A comparative study of retinal topography. *Brain, Behavior and Evolution*, 50:335–346.

Dunning, M. (1998). *Systematics and Biogeography of Cephalopods*, chapter A review of the systematics, distribution, and biology of the arrow squid genera *Ommastrephes Orbigny*, 1835. *Sthenoteuthis Verrill*, 1880, and *Ornithoteuthis okada*, 1927 (Cephalopoda: Ommastrephidae), pages 425–433. Smithsonian Contributions to Zoology.

Gartner, Jr., J. V., Hopkins, T., Baird, R., and Milliken, D. (1987). The lanternfishes of the eastern Gulf of Mexico. *Fishery Bulletin, United States*, 85:81–98.

Haddock, S. H. D. and Case, J. F. (1999). Bioluminescence spectra of shallow and deep-sea gelatinous zooplankton: ctenophores, medusae and siphonophores. *Marine Biology*, 133:571–582.

Haedrich, R. L. and Craddock, J. E. (1968). Distribution and biology of the opisthoproctid fish *Winteria telescopa* brauer 1901. *Brevoria, Museum of Comparative Zoology*, 294:1–11.

Harbison, G., Madin, L., and Swanberg, N. (1978). On the natural history and distribution of oceanic ctenophores. *Deep Sea Research*, 25(3):233 – 256.

Herring, P. J., Latz, M. I., Bannister, N. J., and widder, E. A. (1993). Bioluminescence of the poecilostomatoid copepod *Oncaea conifera*. *Marine ecology progress series*, 94:297–309.

Hopkins, T. L. and Baird, R. C. (1985). Feeding ecology of four hatchetfishes (Sternoptychidae) in the eastern Gulf of Mexico. *Bulletin of Marine Science*, 36(2):260–277.

Jagger, W. S. (1996). Image formation by the crystalline lens and eye of the rainbow trout. *Vision Research*, 36(17):2641–2655.

Jerlov, N. G. (1976). *Marine Optics*. Elsevier.

Johnsen, S. (2001). Hidden in plain sight: The ecology and physiology of organismal transparency. *The Biological Bulletin*, 201(3):301–318.

Johnsen, S., Widder, E. A., and Mobley, C. D. (2004). Propagation and perception of bioluminescence: Factors affecting counterillumination as a cryptic strategy. *Biol Bull*, 207:1–16.

Khorramshahi, O., Schartau, J. M., and Kröger, R. H. (2008). A complex system of ligaments and a muscle keep the crystalline lens in place in the eyes of bony fishes (teleosts). *Vision Research*, 48(13):1503–1508.

Land, M. F. (1982). Scanning eye movements in a heteropod mollusc. *Journal of Experimental Biology*, 96(1):427–430.

Land, M. F. and Nilsson, D.-E. (2002). *Animal eyes*. Animal Biology Series, Oxford.

Latz, M., Frank, T., and Case, J. (1988). Spectral composition of bioluminescence of epipelagic organisms from the Sargasso Sea. *Marine Biology*, 98:441–446.

Laughlin, S. B., de Ruyter van Steveninck, R. R., and Anderson, J. C. (1998). The metabolic cost of neural information. *Nature*, 1:36–41.

Loew, E., McFarland, W., Mills, E., and Hunter, D. (1993). A chromatic action spectrum for planktonic predation by juvenile yellow perch, *Perca flavescens*. *Canadian Journal of Zoology*, 71(2):384–386.

Lythgoe, J. (1979). *The Ecology of Vision*. Clarendon Press, Oxford.

Lythgoe, J. (1984). Visual pigments and environmental light. *Vision Research*, 24:1539–1550.

Mandelman, T. and Sivak, J. G. (1983). Longitudinal chromatic aberration of the vertebrate eye. *Vision Research*, 23(2):1555–1559.

Marshall, N. B. (1971). *Explorations in the Life of Fishes*. Harvard University Press, Cambridge.

Marshall, N. B. (1979). *Developments in Deep-Sea Biology*. Blandford Press, Poole, U.K.

Matthiessen, L. (1882). Ueber die beziehungen, welche zwischen dem brechungsindex des kerncentrums der krystalllinse und den dimensionen des auges bestehen. *Pflüger's Archiv*, 27:510–523.

Matthiessen, L. (1886). Ueber den physikalisch-optischen bau des auges der cetaceen und der fische. *Pflüger's Archiv*, 38:521–528.

Maxwell, J. (1854). Some solutions of problems 2. *Cambridge and Dublin Mathematical Journal*, 8:188–195.

Mayer, A. G. (1912). *Ctenophores of the Atlantic Coast of North America*. Carnegie Institution of Washington, Washington, DC.

Muntz, W. (1976). On yellow lenses in meso pelagic animals. *Journal of the Marine Biological Association of the United Kingdom*, 56(4):963–976.

Muntz, W. (1990). *Stimulus, Environment and Vision in Fishes*, pages 491–511. Chapman & Hall, New York.

Pafort-van Iersel, T. (1983). Distribution and variation of carinariidae and pterotracheidae (heteropoda, gastropoda) of the Amsterdam Mid-north Atlantic Plankton Expedition 1980. *Beaufortia*, 33:73–96.

Parin, N. V. and Borodulina, O. D. (1995). A preliminary review of the *Astronesthes chrysophekadion* species complex assigned to the subgenus *Stomianodon* bleeker, with description of a new species. *Journal of Ichthyology*, 35:21–39.

Pumphrey, R. J. (1961). *Concerning Vision*. Cambridge University Press, London.

Roper, C., C. C., L., and Vecchione, M. (1998). *Systematics and Biogeography of Cephalopods*, chapter Systematics and distribution of *Illex* species; a reVision (Cephalopoda, Ommastrephidae), pages 586:405–423. Smithson. Contr. Zool.

Shand, J., Døving, K. B., and Collin, S. P. (1999). Optics of the developing fish eye: comparisons of Matthiessen's ratio and the focal length of the lens

in the black bream *Acanthopagrus butcheri* (Sparidae, Teleostei). *Vision Research*, 39(6):1071–1078.

Sivak, J. G. and Luer, C. A. (1991). Optical development of the ocular lens of an elasmobranch *Raja eglanteria*. *Vision Research*, 31(3):373–382.

Sutton, T. T. (2003). *Grzimek's Animal Life Encyclopedia, vols. 4–5, second ed.: Fishes I–II*, chapter Stomiiformes (Dragonfishes and relatives), pages 421–430. Thomson-Gale, New York.

Sutton, T. T. (2005). Trophic ecology of the deep-sea fish *Malacosteus niger* (pisces: Stomiidae): An enigmatic feeding ecology to facilitate a unique visual system? *Deep Sea Research Part I: Oceanographic Research Papers*, 52:2065–2076.

Sutton, T. T. and Hopkins, T. L. (1996). Species composition, abundance, and vertical distribution of the stomiid (Pisces: Stomiiformes) fish assemblage of the Gulf of Mexico. *Bulletin of Marine Science*, 59(3):530–542.

Sutton, T. T., Porteiro, F., Heino, M., Byrkjedal, I., Langhelle, G., Anderson, C., Horne, J., Søiland, H., Falkenhaug, T., Godø, O., and Bergstad, O. (2008). Vertical structure, biomass and topographic association of deep-pelagic fishes in relation to a mid-ocean ridge system. *Deep Sea Research Part II: Topical Studies in Oceanography*, 55:161–184.

Sutton, T. T., Wiebe, P. H., Madin, L., and Bucklin, A. (2010). Diversity and community structure of pelagic fishes to 5000 m depth in the Sargasso Sea. *Deep Sea Research Part II: Topical Studies in Oceanography*, 57:2220–2233.

Wagner, H. J., Frohlich, E., Negishi, K., and Collin, S. P. (1998). The eyes of deep-sea fish II functional morphology of the retina. *Progress in retinal and eye Research*, 17:637–685.

Walls, G. L. (1942). *The vertebrate eye and its adaptive radiation*. New York, Hafner, New York.

Warrant, E. J. (1999). Seeing better at night: life style, eye design and the optimum strategy of spatial and temporal summation. *Vision Research*, 39(9):1611–1630.

Warrant, E. J. (2000). The eyes of deep-sea fishes and the changing nature of visual scenes with depth. *Philosophical Transactions of the Royal Society of London. Series B: Biological Sciences*, 355(1401):1155–1159.

Warrant, E. J., Collin, S. P., and Locket, N. A. (2003). *Sensory Processing in Aquatic Environments*, chapter Eye Design and Vision in Deep-Sea Fishes, pages 303–322. Springer-Verlag New York Inc.

Warrant, E. J. and Locket, N. A. (2004). Vision in the deep sea. *Biological Reviews*, 79(3):671–712.

Waterman, T. (1981). *Polarization Sensitivity*, pages 281–469. Springer, New York.

www.fishbase.org, v. . (2012). *FishBase*. World Wide Web electronic publication.

Young, R. E. (1978). Vertical distribution and photosensitive vesicles of pelagic cephalopods from Hawaiian waters. *Fish. Bull.*, 76:583–615.

Young, R. E. and Hirota, J. (1998). *Contributed papers to the international symposium on large pelagic squids*, chapter Review of the ecology of *Sthenoteuthis oualaniensis* near the Hawaiian Archipelago, pages 132–133. Japan Marine Fishery Resources Research Center, Tokyo.

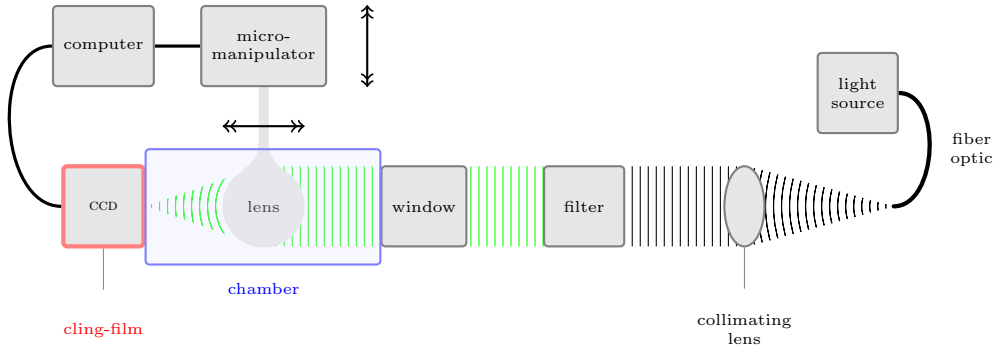

Figure 1: An illustration of the optical setup used to measure the point spread function (PSF) of marine animal lenses. While the cling-film protected CCD registers focused images of the point source, the computer controls the axial distance of the biological lens submerged in the chamber. By scanning the focal point the optimal focal distance was estimated. All the dimensions of this setup are mentioned in the text.

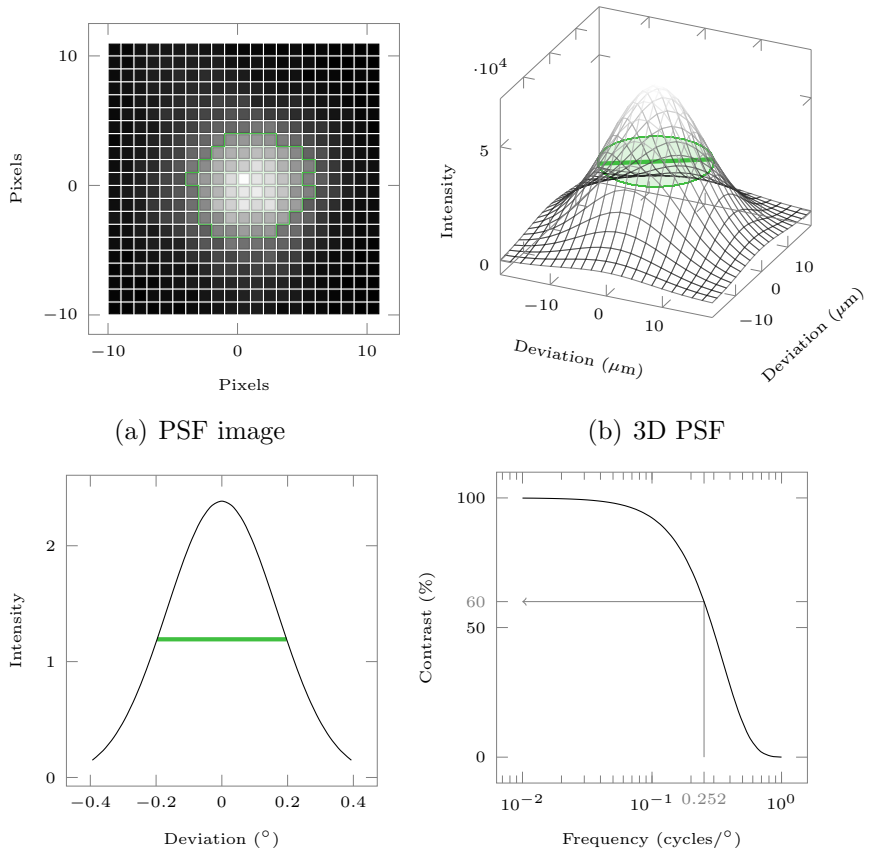

(a) PSF image (b) 3D PSF

(c) 2D PSF (d) MTF

Figure 2: An illustration of the various steps in calculating visual acuity in this study. (a) An example image of the Point Spread Function (PSF) of *Melanolagus bericoides*. x & y-axes are in pixels (each pixel is 2.2×2.2 μm). The area that contained pixels larger than half the maximum intensity (i.e. 65536/2) is highlighted in green. (b) The three dimensional representation of the PSF image. The x & y-axes are in μm and denote the distance from the lens optical axis while the z-axis is image intensity. The highlighted disk has the same area as the one in the PSF image and is at the mid point between the PSF's smallest and largest values (i.e. 32767.5). The disk's diameter (green line) equals the Full Width at Half Maximum (FWHM) of the PSF. (c) A two dimensional PSF with an $\angle$FWHM (green line) equivalent to the FWHM as before (equal to the arcsin of the FWHM divided with the focal length of *M. bericoides*). The x-axis is deviation from the optical axis in degrees and the y-axis is relative intensity. (d) The Modulation Transfer Function (MTF) of *M. bericoides*'s lens. The x-axis is spatial frequency in cycles per degree in log-scale and the y-axis is perceived image contrast. The MTF was calculated by applying a Fourier Transform on the PSF. As an example, a hypothetical cutoff frequency of 0.252 cycles/° is marked and shows that the contrast at that maximal retinal resolution is 60%.

Table 1: The number of replicates (n_{animal}), total number of lenses (n_{lens}), mean and standard deviation of the lens radius (R), focal length (f), and f-number ($f/\#$), as well as the full width at half maximum (FWHM), angular full width at half maximum ($\angle$FWHM), and daytime depth range for all the species examined in this study. While lens radius was measured for all species-replicates, the other lens parameters were not always measurable for all replicates.

Species	n_{animal}	n_{lens}	R ± sd (mm)	f ± sd (mm)	$f/\#$ ± sd	FWHM (μm)	$\angle$FWHM(°)	Depth (m)
Actinopterygii								
Anoplogaster cornuta	1	2	1.3 ± 0.01	3.4 ± 0.61	1.3 ± 0.22	6.1	0.12	750–2300[1]
Argyropelecus aculeatus	4	6	1.7 ± 0.32	3.8 ± 0.82	1.2 ± 0.049	6.1	0.13	350–450[2]
Astronesthes lucifer	1	2	1.4 ± 0.0088	2.8 ± 0.062	1 ± 0.016	6.1	0.12	185–560[3]
Avocettina infans	2	3	0.92 ± 0.025	1.5 ± 0.59	0.82 ± 0.3	4.3	0.12	600–2000[4]
Benthosema suborbitale	9	14	1.5 ± 0.13	3.2 ± 0.31	1 ± 0.1	4.3	0.08	400–600[5]
Caranx bartholomaei	1	1	1.4	2.3	0.81	15	0.38	0–50[4]
Chauliodus sloani	1	2	1.4 ± 0.0089	2.9 ± 0.26	1 ± 0.086	11	0.23	500–2800[6]
Cheilopogon sp.	1	1	9.4	-	-	19	-	1–5[4]
Coccorella atlantica	1	1	1.4	2.1	0.78	13	0.34	500–1000[4]
Diaphus splendidus	1	1	1.5	-	-	12	-	300–600[5]
Diplospinus multistriatus	1	2	1.1 ± 0.0022	2 ± 0.02	0.94 ± 0.0076	7.4	0.21	500–1000[4]
Gonostoma elongatum	3	5	1 ± 0.23	2 ± 0.15	1.1 ± 0.21	4.3	0.13	500–1200[7]
Idiacanthus antrostomus	1	2	0.97 ± 0.024	1.9 ± 0.097	0.96 ± 0.026	5	0.16	500–2000[8]
Lepidophanes guentheri	6	6	1.5 ± 0.55	3.7 ± 1.1	1 ± 0.042	14	0.31	400–900[5]
Malacosteus niger	3	5	1.6 ± 0.41	3.3 ± 0.86	1.1 ± 0.14	7	0.18	500–900[9]
Melanolagus bericoides	2	4	2.6 ± 0.1	5.5	1	19	0.2	750–1700[1]
Opisthoproctus soleatus	2	2	2.7 ± 0.29	6.7 ± 0.62	1.2 ± 0.015	11	0.087	500–700[4]
Regalecus glesne	1	2	0.64 ± 0.0047	2.1 ± 0.04	1.6 ± 0.02	6.1	0.17	0–200[4]
Saccopharynx sp.	1	2	0.47 ± 0.0077	-	-	74	-	1000–3000[10]
Scopeloberyx robustus	1	1	1.3	2.4	0.92	8.6	0.2	750–2300[1]
Scopelosaurus hoedti	1	2	1.6 ± 0.0062	3.4 ± 0.011	1 ± 0.0072	5.6	0.094	300–600[4]
Selar crumenophthalmus	1	2	1.4 ± 0.013	2.5 ± 0.71	0.89 ± 0.25	12	0.35	0–170[4]
Sternoptyx diaphana	12	20	1.2 ± 0.18	2.7 ± 0.45	1.1 ± 0.12	4.3	0.089	700–1200[11]
Taaningichthys bathyphilus	1	1	1.1	-	-	11	-	1000–1550[5]
Cephalopoda								
Chiroteuthis sp.	1	2	1.6 ± 0.095	-	-	130	-	700–800[12]
Galiteuthis pacifica	1	3	1.1 ± 0.085	2.2 ± 0.16	0.99 ± 0.065	4.3	0.12	600–800[12]
Illex sp.	2	3	1.4 ± 0.14	2.4 ± 0.82	0.89 ± 0.27	11	0.29	200–600[13]
Pterygioteuthis microlampus	2	4	1 ± 0.26	1.7 ± 0.35	0.84 ± 0.2	3.5	0.15	300–600[12]
Sthenoteuthis oualaniensis	1	2	4.3 ± 0.062	10 ± 0.4	1.2 ± 0.063	17	0.093	400–600[14]
Gastropoda								
Pterotrachea coronata	8	10	0.61 ± 0.043	0.87 ± 0.38	0.72 ± 0.32	3.5	0.21	100–1000[15]

[1] Sutton et al., 2008 [2] Hopkins and Baird, 1985 [3] Parin and Borodulina, 1995 [4] www.fishbase.org, 2012 [5] Gartner et al., 1987
[6] Sutton et al., 2008, 2010, Sutton and Hopkins, 1996 [7] Sutton et al., 2010 [8] Sutton, 2003 [9] Sutton, 2005 [10] Bertelsen and Nielsen, 1986
[11] Hopkins and Baird, 1985, Sutton et al., 2010 [12] Young, 1978 [13] Roper et al., 1998 [14] Young and Hirota, 1998, Dunning, 1998
[15] Pafort-van Iersel, 1983

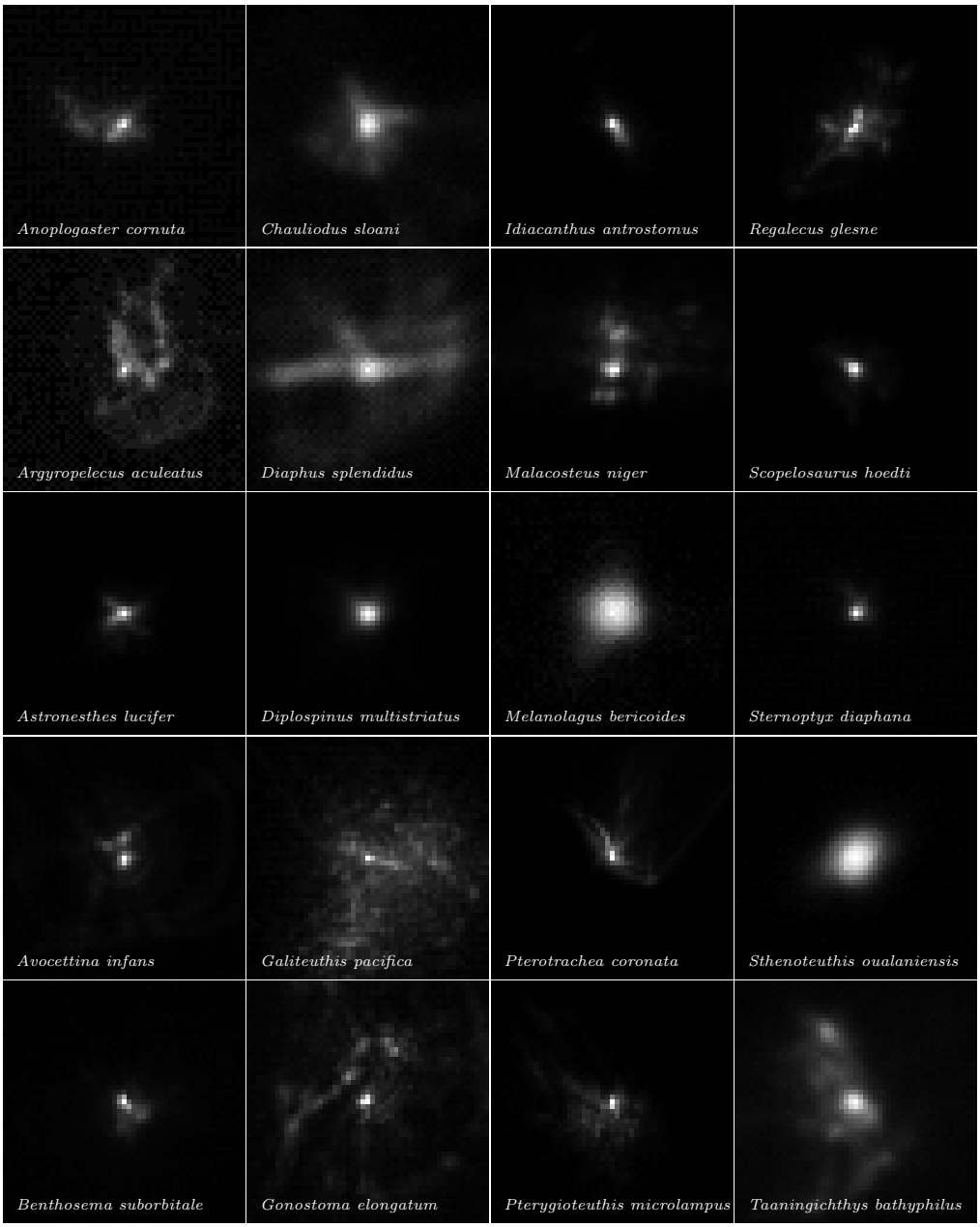

Figure 3: Close-up images of point spread functions (PSF) from a selection of animal lenses. Each PSF's maximal pixel value was equalized between PSFs for easier visual inspection. The image size is 50×50 pixels, and the pixel size is 2.2×2.2 μm (so each pane width and/or height is 110 μm).

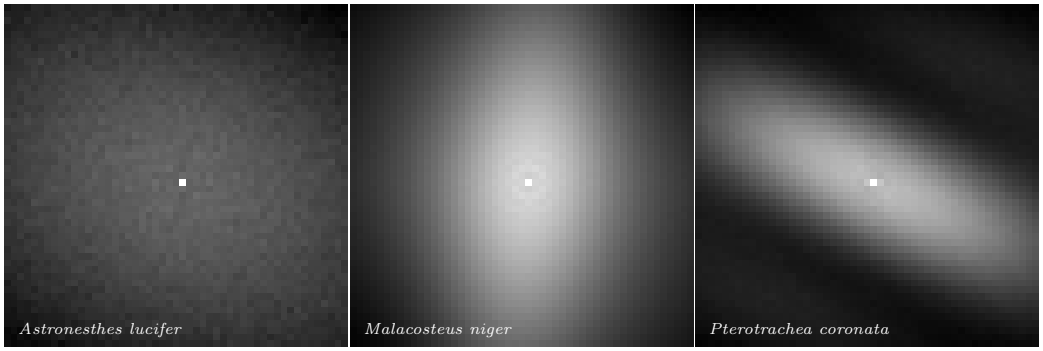

Figure 4: Close-up images of the modulation transfer function (MTF) of *Astronesthes lucifer*, *Malacosteus niger*, and *Pterotrachea coronata*. High intensity values correspond to high contrast and vice versa. Contrast at the image-center relates to low spatial frequencies (i.e. coarse details), and contrast at its periphery relates to high spatial frequencies (i.e. finer details). The image size is 50×50 pixels, and each pixel corresponds to 0.46 cycles per μm.

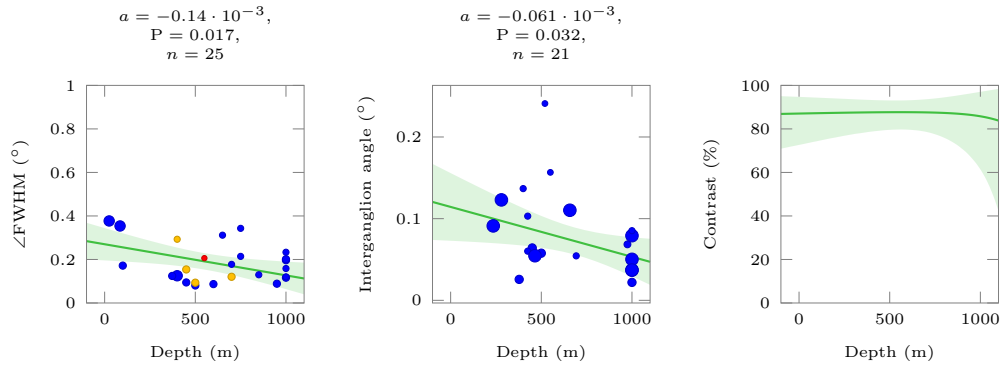

(a) (b) (c)

Figure 5: Visual acuity in pelagic animals. (a) Full Width at Half Maximum of angular Point Spread Functions (∠FWHM) in degrees of pelagic fishes and mollusk lenses against mean daytime depth in meters. The markers of Actinopterygii, Cephalopoda, and Gastropoda are colored blue, orange, and red respectively. (b) Angular separation of inter retinal ganglion cells in degrees of pelagic fishes against mean daytime depth in meters (data taken from Wagner et al. (1998)). The regressors were weighted by the inverse of the depth interval each animal occupied (denoted by the size of the markers: small markers had less weight than large ones). The linear regression and its 95% confidence interval are denoted by the green line and shaded area. The slope, P value of the regression, and number of species are displayed in the title. (c) Perceived image contrast at the cutoff frequency of pelagic fishes retinas as a function of daytime depth in meters. Contrast was calculated at the cutoff frequency taken from the regression in (b) using the ∠FWHM regression from (a).